DEVELOPMENTAL DYNAMICS 239:211–221, 2010

SPECIAL ISSUE RESEARCH ARTICLE

Delayed Dopaminergic Neuron Differentiation in *Lrp6* Mutant Mice

Gonçalo Castelo-Branco,[1†‡] Emma R. Andersson,[1†§] Eleonora Minina,[2†] Kyle M. Sousa,[1◇] Diogo Ribeiro,[1] Chikara Kokubu,[3] Kenji Imai,[2] Nilima Prakash,[2] Wolfgang Wurst,[2,4]* and Ernest Arenas[1]*

Wnts are known to bind and activate multiple membrane receptors/coreceptors and to regulate dopaminergic (DA) neuron development and ventral midbrain (VM) morphogenesis. The low density lipoprotein receptor–related protein (Lrp6) is a Wnt co-receptor, yet it remains unclear whether *Lrp6* is required for DA neuron development or VM morphogenesis. *Lrp6* is expressed ubiquitously in the developing VM. In this study, we show that *Lrp6*$^{-/-}$ mice exhibit normal patterning, proliferation and cell death in the VM, but display a delay in the onset of DA precursor differentiation. A transient 50% reduction in tyrosine hydroxylase–positive DA neurons and in the expression of DA markers such as *Nurr1* and *Pitx3*, as well as a defect in midbrain morphogenesis was detected in the mutant embryos at embryonic day 11.5. Our results, therefore, suggest a role for *Lrp6* in the onset of DA neuron development in the VM as well as a role in midbrain morphogenesis. *Developmental Dynamics 239:211–221, 2010.* © 2009 Wiley-Liss, Inc.

Key words: Lrp; Wnt; dopaminergic; neurogenesis, precursor; midbrain

Accepted 5 August 2009

INTRODUCTION

Wnts comprise a family of 19 secreted lipid-modified glycoproteins that regulate a myriad of biological processes including midbrain and dopaminergic (DA) neuron development (McMahon and Bradley, 1990; Thomas and Capecchi, 1990; Castelo-Branco et al., 2003; Prakash et al., 2006; Andersson et al., 2008). We have previously shown that canonical Wnt signaling, leading to the stabilization of cytosolic β-catenin (Logan and Nusse, 2004), is involved in the differentiation of postmitotic DA precursors into DA neurons (Castelo-Branco et al., 2004), and Wnt5a, which activates Rac1, is involved in DA differentiation and

Additional Supporting Information may be found in the online version of this article.

[1]Laboratory of Molecular Neurobiology, Medical Biochemistry and Biophysics, Karolinska Institutet, Stockholm, Sweden
[2]Helmholtz Centre Munich, German Research Centre for Environmental Health, and Technical University Munich, Institute of Developmental Genetics, Deutsches Zentrum für Neurodegenerative Erkrankungen (DZNE), Munich/Neuherberg, Germany
[3]Center for Advanced Science and Innovation, Osaka University, Osaka, Japan
[4]Max Planck Institute of Psychiatry, Munich, Germany

Grant sponsor: Swedish Research Council; Grant number: VR2008 and 2811 and DBRM; Grant sponsors: Swedish Foundation for Strategic Research (INGVAR and CEDB), Norwegian Research Council, Karolinska Institutet, Michael J Fox Foundation, European Union (Eurostemcell); Grant sponsor: BMBF National Genome Research; Grant number: FKZ 01GS08174; Grant sponsor: Virtual Institute on Neurodegeneration and Ageing; Grant number: VH-VI-252; Grant sponsor: Initiative and Networking Fund in the framework of the Helmholtz Alliance of Systems Biology and of Mental Health in an Ageing Society; Grant number: HA-215; Grant sponsor: Bayerischer Forschungsverbund 'ForNeuroCell'; Grant number: F2-F2410-10c/20697; Grant sponsor: European Union; Grant numbers: mdDANEURODEV FP7-Health-2007-B-222999, EuTRACC LSHG-CT-2006-037445; Deutsche Forschungsgemeinschaft (DFG); Grant numbers: SFB 596, WU 164/3-2, WU 164/4-1.

†Drs. Castelo-Branco, Andersson, and Minina contributed equally to this work.
‡Dr. Castelo-Branco's present address is The Wellcome Trust/CRUK Gurdon Institute, University of Cambridge, Tennis Court Road, Cambridge CB2 1QN, United Kingdom.
§Dr. Andersson's present address is Department of Cell and Molecular Biology, Karolinska Institute, 17177 Stockholm, Sweden.
◇Dr. Sousa's present address is Department of Molecular and Integrative Physiology, University of Michigan Medical School, Ann Arbor, MI 48109-0622.
***Correspondence to: Ernest Arenas, Karolinska Institutet, Scheeles vag 1, A1, plan 2, 17177 Stockholm Sweden. E-mail: ernest.arenas@ki.se and Wolfgang Wurst, Institute of Developmental Genetics, Munich/Neuherberg, Germany. E-mail: wurst@helmholtz-muenchen.de**

DOI 10.1002/dvdy.22094
Published online 30 September 2009 in Wiley InterScience (www.interscience.wiley.com).

midbrain morphogenesis (Andersson et al., 2008). Wnt1 plays an essential role in the development of the mid-/hindbrain region and in the establishment of the DA progenitor domain in the ventral midbrain (VM; McMahon and Bradley, 1990; Thomas and Capecchi, 1990; Danielian and McMahon, 1996; Panhuysen et al., 2004; Prakash et al., 2006).

Wnt signaling is transduced by a receptor complex consisting of the seven-pass transmembrane Frizzled (Fzd) receptors and the low density lipoprotein receptor (LDLR) -related protein (Lrp) 5 or 6 (Tamai et al., 2000; Mao et al., 2001; Cong et al., 2004). Initially, observations that *Drosophila* mutants for *arrow*, an ortholog of the mammalian *Lrp6*, phenocopy the *wingless* (the Wnt1 *Drosophila* ortholog) mutants, supported Lrp as an exclusive canonical Wnt signaling component (Wehrli et al., 2000). However, the involvement of *Lrp6* in modulating planar cell polarity (PCP) and convergent extension (CE) has recently been described in both *Xenopus* (Tahinci et al., 2007) and mice (Bryja et al., 2009), indicating that Lrp6 could potentially regulate DA neuron development through multiple signaling mechanisms. In support of this hypothesis, we recently found that Wnt5a, a Wnt that induces PCP signals, also regulates DA neuron development in vivo (Andersson et al., 2008). These results suggest that *Lrp6* could potentially modulate multiple aspects of DA neuron development through different Wnt ligands. In this study, we asked whether *Lrp6* is required for midbrain or DA neuron development in vivo, by analyzing VM, progenitor and neuron development and midbrain morphogenesis in $Lrp6^{-/-}$ mice.

RESULTS

Lrp Coreceptors Are Expressed in the Developing VM

Wnts transduce their signal through a ternary complex formed by receptors of the Fzd and Lrp families (Logan and Nusse, 2004). The developing VM is known to express several Fzd receptors (Rawal et al., 2006; Fischer et al., 2007), while the ubiquitous central nervous system expression of *Lrp* coreceptors has been shown in both *Xenopus* and mouse (Houston and Wylie, 2002; Zhou et al., 2004a). We first confirmed these results during rat and mouse VM development by quantitative polymerase chain reaction (qPCR) and in situ hybridization. *Lrp5* and *Lrp6* transcripts were detected in the developing VM by qPCR (Fig. S1A,B), and in situ hybridization confirmed that *Lrp5* and *Lrp6* were ubiquitously expressed at embryonic day (E) 11.5 (Supp. Fig. S1C, which is available online).

$Lrp6^{-/-}$ Mice Do Not Display Patterning, Proliferation, or Cell Death Defects in the Ventral Midbrain

Several developmental phenotypes associated with dysregulation of Wnt signaling have been described in $Lrp6^{-/-}$ mice, including a deletion of the dorsocaudal midbrain and cerebellar defects (Pinson et al., 2000). Interestingly, whereas the isthmus was clearly less well-defined at a dorsal level in E9.5 and E10.5 $Lrp6^{-/-}$ mice (Fig. 1A,B, and Pinson et al., 2000), in situ hybridization revealed no difference in the ventral expression of *Otx2*, *Engrailed* (*En1*), *Lmx1b*, *Sonic Hedgehog* (*Shh*) or *Wnt5a* in the midbrain of E9.5 (Fig. 1A) or E10.5 (Fig. 1B) $Lrp6^{-/-}$ mice. Previous observations by Pinson et al. were confirmed by decreased or lost dorsal expression of midbrain/hindbrain marker genes, such as *En1* and *Fibroblast growth factor 8* (*Fgf8*), and concomitant loss of dorsal mid-/hindbrain tissue at E12.5 (Fig. 1C). However, ventral expression of *En1* and *Fgf8* at the midbrain–hindbrain boundary (MHB) was normal (Fig. 1C). As previously reported (Pinson et al., 2000), many $Lrp6^{-/-}$ embryos displayed neural tube defects, including exencephaly. When patterning was examined in exencephalic $Lrp6^{-/-}$ mice, *Shh* (marker for floor plate [FP]/basal plate [BP]), *Lmx1b* (FP and roof plate [RP]) and *Wnt3a* (RP) were expressed in the correct structures at E9.5 (Supp. Fig. S2A) and E10.5 (Supp. Fig. S2B). Thus, despite the dorsal mid–hindbrain defects in $Lrp6^{-/-}$ mice, no discernible patterning defects manifested in the VM.

In agreement with our findings on patterning, we did not observe any decrease in the proliferation of VM precursors at E11.5, as assessed by EdU (5-ethynyl-2′-deoxyuridine) incorporation (Fig. 2A,B) immunostaining for the cell cycle marker phospho-histone-3 at E11.5 (Fig. 2C,D), or by BrdU (5-bromo-2-deoxyuridine) incorporation at E10.5, E11.5, E12.5 or E15.5 (Supp. Fig. S3). Moreover, the number of cleaved/active caspase-3 immunoreactive cells, a marker of cells undergoing apoptosis, was similarly low in wild-type and mutant VM at E11.5 (Supp. Fig. S4) and E13.5 (data not shown). The expression level and distribution of the neural stem/progenitor cell marker nestin (Fig. 2D,E) and the mRNA levels of the DA progenitor cell marker, *aldehyde dehydrogenase 2* (*AHD2*; Fig. 2F), expressed from E9.5 onward (Wallen et al., 1999), were not altered in the mutant VM. These results suggested that deletion of *Lrp6* does not alter normal patterning, proliferation, or cell survival in the VM, including the DA lineage.

Altered VM Morphology in $Lrp6^{-/-}$ Mice

We have previously shown that *Wnt5a* is required for the appropriate invagination of the VM ventricular zone (VZ) and medial hinge-point formation (Andersson et al., 2008), in that loss of *Wnt5a* leads to a U-shaped, rather than V-shaped, VM. Consequently, $Wnt5a^{-/-}$ mice sometimes display neural tube closure defects (Qian et al., 2007; Andersson et al., 2008). $Lrp6^{-/-}$ mice also present with neural tube closure defects such as exencephaly (Pinson et al., 2000; Bryja et al., 2009; Andersson et al., 2009), which is rescued by loss of *Wnt5a* in a dose-dependent manner (Bryja et al., 2009). We therefore asked how the loss of *Lrp6* itself affects VM VZ morphology.

In contrast to the flattened VM (VZ) medial hinge-point previously reported in $Wnt5a^{-/-}$ mice, $Lrp6^{-/-}$ mice generally displayed a much more acute VM VZ angle of circa 40°,

compared with wild-type mice which displayed a circa 135° VM VZ angle ($P = 0.013$, N = 3, unpaired *t*-test). This resulted in a narrow V-shaped VM VZ in the *Lrp6*$^{-/-}$ mice (Fig. 3A,B).

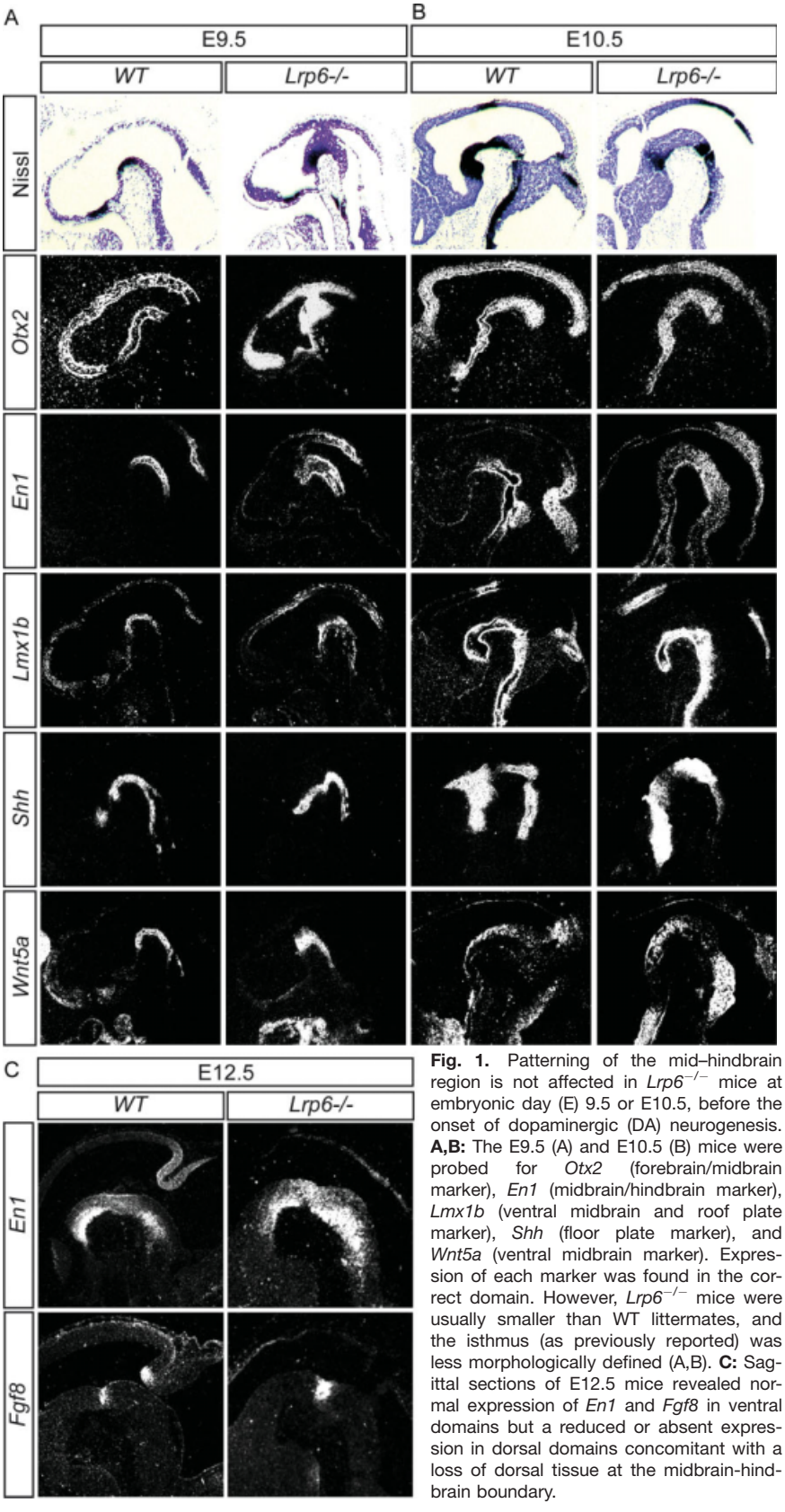

Fig. 1. Patterning of the mid–hindbrain region is not affected in *Lrp6*$^{-/-}$ mice at embryonic day (E) 9.5 or E10.5, before the onset of dopaminergic (DA) neurogenesis. **A,B:** The E9.5 (A) and E10.5 (B) mice were probed for *Otx2* (forebrain/midbrain marker), *En1* (midbrain/hindbrain marker), *Lmx1b* (ventral midbrain and roof plate marker), *Shh* (floor plate marker), and *Wnt5a* (ventral midbrain marker). Expression of each marker was found in the correct domain. However, *Lrp6*$^{-/-}$ mice were usually smaller than WT littermates, and the isthmus (as previously reported) was less morphologically defined (A,B). **C:** Sagittal sections of E12.5 mice revealed normal expression of *En1* and *Fgf8* in ventral domains but a reduced or absent expression in dorsal domains concomitant with a loss of dorsal tissue at the midbrain-hindbrain boundary.

Delayed DA Differentiation in *Lrp6*$^{-/-}$ Mice

Ngn2 is a basic helix–loop–helix transcription factor required for DA neurogenesis (Kele et al., 2006). At E11.5, *Ngn2* expression in the midbrain FP defines the DA progenitor domain, whereas *Ngn1* in the adjacent BP defines the oculomotor (OM) and red nucleus (RN) progenitor domains (Kele et al., 2006). Interestingly, both *Ngn1* and *Ngn2* were expressed in the expected domains, despite the *Lrp6*$^{-/-}$ brains sometimes being smaller (Fig. 4A). This result was further confirmed by qPCR for Ngn2 (Fig. 4B).

Nurr1, a nuclear receptor expressed in postmitotic cells in the VM DA lineage (DA precursors and neurons), is known to be required for the differentiation of DA precursors and the acquisition of the DA phenotype (Zetterstrom et al., 1997; Castillo et al., 1998; Le et al., 1999). At E11.5, we found a 40% decrease in the number of Nurr1+ cells (from 647.7 ± 77.38 in the wild-type (WT) to 391.0 ± 102.8; Fig. 5A,B), and a 60% decrease in *Nurr1* mRNA levels (Fig. 5C). However, these defects were partially recovered as early as E13.5 (Fig. 5D–F). We next examined whether the reduction in *Nurr1* expression and in cell numbers were the result of a delayed marker acquisition or accompanied by delayed differentiation into tyrosine hydroxylase–positive (TH+) DA neurons.

Pitx3 is a transcription factor expressed during DA differentiation (Smidt et al., 1997) that is required for DA neuron maintenance and survival (Hwang et al., 2003; Nunes et al., 2003; van den Munckhof et al., 2003; Smidt et al., 2004; Maxwell et al., 2005). We found that *Pitx3* expression was greatly reduced, as assessed by in situ hybridization at E12.5 (Fig. 6A) and quantitative reverse transcription PCR (qRT-PCR) at E11.5 (Fig. 6B), confirming that the DA neuron differentiation process was impaired.

We next examined the number of TH+ DA neurons at E11.5, and observed a 50% reduction in the number of TH+ cells (362.5 ± 30.38 in WT, 175.5 ± 24.4 in *Lrp6*$^{-/-}$; Fig. 6C,D), with no apparent change in

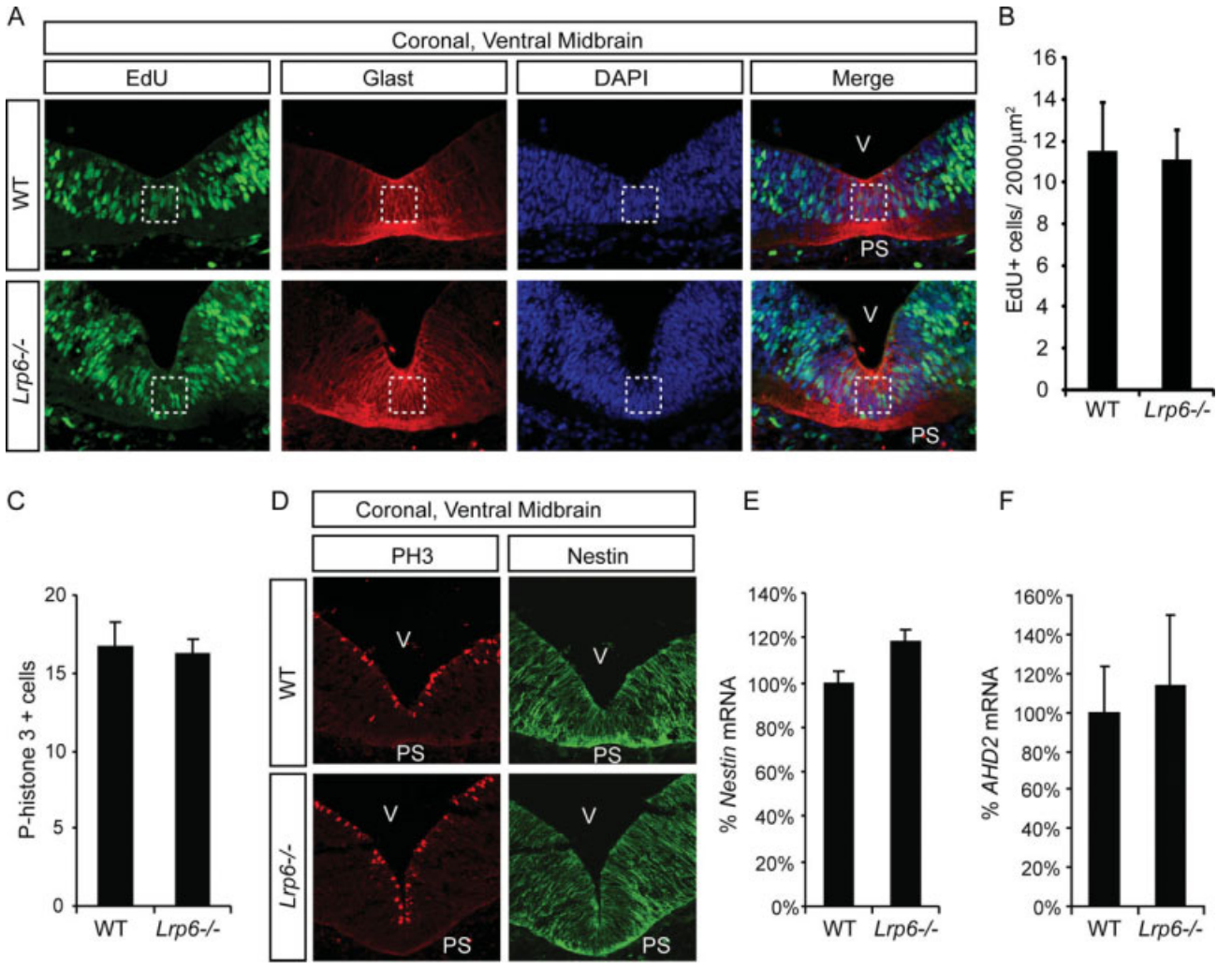

Fig. 2. Proliferation and early dopaminergic (DA) markers are unchanged in *Lrp6*$^{-/-}$ mice. **A:** The proliferative capacity of embryonic day (E) 11.5 ventral midbrain (VM) precursors was not affected in *Lrp6*$^{-/-}$ mice, as assessed by EdU (5-ethynyl-2′-deoxyuridine) staining in coronal sections of the ventral midbrain of 2-hr EdU-pulsed embryos at E11.5. **B:** Quantification of EdU+ cells did not reveal a significant difference between *Lrp6*$^{-/-}$ and wild-type mice within the Glast-expressing floor plate. **C–E:** Quantification of phospho-histone-3 (PH3+) cells (C) after immunostaining of the VM at E11.5 for PH3 and Nestin (D), and *Nestin* quantitative polymerase transcription polymerase chain reaction (qPCR; E) showed no difference in *Lrp6*$^{-/-}$ mice compared with wild-type (WT). **F:** Similarly, qPCR for the DA progenitor marker *AHD2* revealed no difference at E11.5. V, ventricle; PS, pial surface.

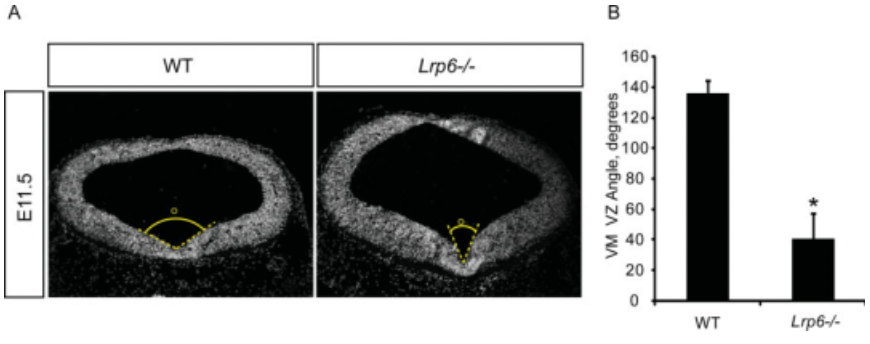

Fig. 3. Loss of *Lrp6* results in an acute ventral midbrain (VM) ventricular zone (VZ) invagination angle. **A:** The angle of invagination was measured on DAPI (4′,6-diamidine-2-phenylidole-dihydrochloride) -stained coronal VM sections. **B:** At embryonic day (E) 11.5, wild-type mice displayed an angle of circa 135°, which was significantly different from the 40° angle seen in *Lrp6*$^{-/-}$ mice (unpaired *t*-test; N = 3; $P = 0.012$).

the total population of neurons in the VM (β-tubulin III [TUJ-1] -positive cells; Fig. 6C). *TH* mRNA levels were also significantly lower in *Lrp6*$^{-/-}$ mice, as assessed by qPCR (Fig. 6E) and in situ hybridization (data not shown). However, at E13.5, the decrease in the number of TH+ cells in the *Lrp6*$^{-/-}$ mice was attenuated, and a reduction of only 25% was detected (Fig. 6F,G). No statistically significant difference in *TH* mRNA levels was detected by qPCR at this stage (Fig. 6H). Moreover, at E17.5, the numbers of TH+ cells were normal in the substantia nigra and in the ventral tegmental area, and their

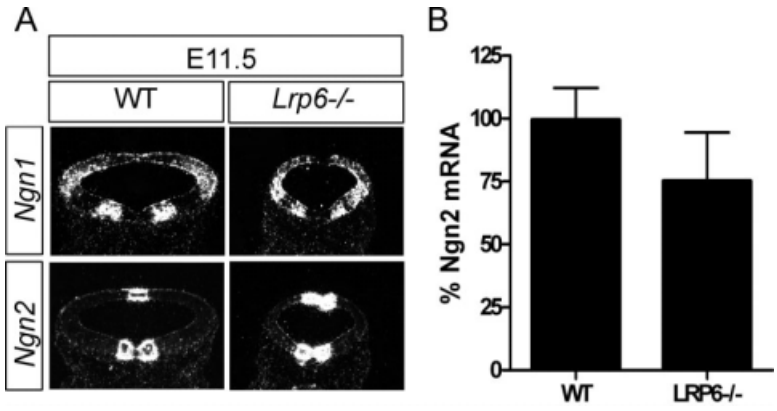

Fig. 4. Ventral midbrain expression of *Ngn1* and *Ngn2* is normal in *Lrp6*$^{-/-}$ mice. **A:** *Ngn1* and *Ngn2* were expressed normally in the midbrain of *Lrp6*$^{-/-}$ mice at embryonic day (E) 11.5, as assessed by in situ hybridization. **B:** qPCR did not reveal a statistically significant difference in *Ngn2* mRNA levels in the VM.

innervation of the striatum was also normal in *Lrp6*$^{-/-}$ mice (data not shown).

These data suggest that the alteration in the number of Nurr1 and TH+ cells during E11.5–E13.5 was the result of a delay in the differentiation of DA precursors and DA neurons in the mutant VM.

DISCUSSION

In this study, we examined whether the Wnt coreceptor, *Lrp6*, is required for VM DA neuron development or midbrain morphogenesis. Whereas the function of *Lrp6* in the developing ventral midbrain has not yet been described, *Lrp6* has previously been found to be necessary for isthmus and dorsocaudal midbrain development (Pinson et al., 2000). We report here that Lrp6 is required for the timely onset of DA differentiation in the VM and normal VM morphogenesis, but not for the proper patterning, growth, and survival of VM tissue.

Wnt1 (a β-catenin–activating Wnt) has been shown to be essential for both dorsal and ventral midbrain development, including DA neuron development (McMahon and Bradley, 1990; Thomas and Capecchi, 1990; Danielian and McMahon, 1996; Panhuysen et al., 2004; Prakash et al., 2006). Moreover, we have previously shown that other Wnts can also contribute to the development of DA neurons in vivo and in vitro (Castelo-Branco et al., 2003; Andersson et al., 2008). When the specific contribution made by *Lrp6* to DA neuron development was examined in vivo, we found that the *Lrp6* receptor was required for the timely onset of DA differentiation in the VM. *Ngn2* and *Ahd2* mRNA levels were normal in *Lrp6*$^{-/-}$ mice, indicating that the delay in differentiation occurs after onset of expression of these markers in DA progenitors. Indeed, the most significant difference that we detected was a decrease in the expression of *Pitx3*, a gene with an important role in DA differentiation (Hwang et al., 2003; Nunes et al., 2003; van den Munckhof et al., 2003; Smidt et al., 2004; Maxwell et al., 2005). This defect was accompanied by a decrease in the number of Nurr1+ precursors and TH+ DA neurons, as well as lower expression of *Nurr1* and *TH* mRNAs at E11.5 in the VM of *Lrp6*$^{-/-}$ mice. These effects were specific to the DA lineage, in that no differences in cell death, proliferation, or patterning were observed in the mutant VM, despite the fact that these processes are also regulated by Wnts (McMahon and Bradley, 1990; Thomas and Capecchi, 1990; Pinson et al., 2000; Castelo-Branco et al., 2003; Viti et al., 2003; Panhuysen et al., 2004; Ciani and Salinas, 2005). Thus, our results suggest a role for Lrp6 in the differentiation of DA neurons during early stages of their development.

Compared with *Wnt1*$^{-/-}$ mice, the DA differentiation defect in *Lrp6*$^{-/-}$ mice was transient, while *Wnt1*$^{-/-}$ mice show a severe and permanent defect (McMahon and Bradley, 1990; Thomas and Capecchi, 1990; Prakash et al., 2006). Moreover, the decrease in expression of Pitx3 was more severely affected in the *Wnt1*$^{-/-}$ mice (Prakash et al., 2006) than in the *Lrp6*$^{-/-}$ mice. These results suggest the presence of compensatory mechanisms that permit a recovery of postmitotic DA precursors and neurons in the *Lrp6*$^{-/-}$ mice. One possibility is that Lrp5, another canonical Wnt coreceptor expressed in the VM, may be able to compensate for the absence of *Lrp6*. In support of this hypothesis, *Lrp5*$^{+/-}$;*Lrp6*$^{-/-}$ mice exhibit a much more severe phenotype than *Lrp6*$^{-/-}$ mice, but die before DA neurogenesis (Kelly et al., 2004), thus precluding the analysis of DA neuron development in these mice. Future experiments using midbrain-specific deletions of these genes would help to further elucidate the specific contribution of Lrp receptors to Wnt signaling in the VM.

Region-specific defects in the *Lrp6*$^{-/-}$ mice have also been observed in brain areas other than the VM. Neuronal development is severely affected in the dorsal thalamus (with ablation of *Shh* and *Wnt5a* expression), and in the dentate gyrus of *Lrp6*$^{-/-}$ mice (Zhou et al., 2004b), while other hippocampal and neocortical cell types are not affected (Zhou et al., 2004b). These data, together with our results showing a developmental impairment of a ventral neuronal cell type in the midbrain, suggest a function of *Lrp6* as a regulator of neuronal development in specific cell lineages. Interestingly, in the first study by Zhou et al. (Zhou et al., 2004a), a disruption of thalamocortical projections was described. We therefore examined the innervation of the striatum of *Lrp6*$^{-/-}$ mice at E17.5, aiming at detecting a possible permanent defect in the nigrostriatal pathway, but did not find any alterations.

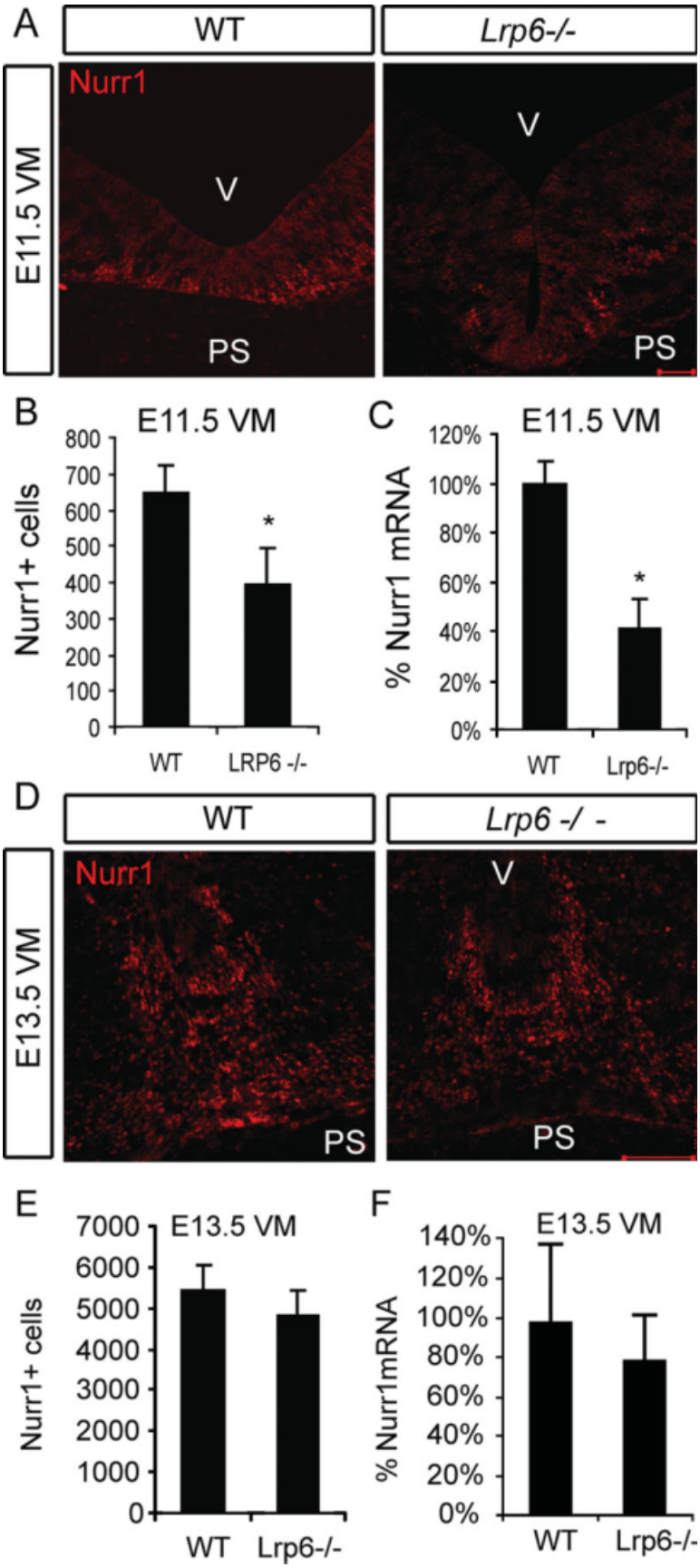

Fig. 5. Postmitotic cells in the dopaminergic lineage are reduced at embryonic day (E) 11.5, but recover by E13.5, in *Lrp6*$^{-/-}$ mice. **A,B:** The number of Nurr1+ precursors was assessed by immunohistochemistry and was reduced from 647 ± 77.38 in wild-type to 391 ± 102.8 in the *Lrp6*$^{-/-}$ mice (paired *t*-test; N = 3; $P = 0.0136$). **C:** qPCR analysis of ventral midbrains (VMs) from *Lrp6*$^{-/-}$ mice revealed a similar decrease in *Nurr1* mRNA levels (paired *t*-test; N = 6; $P = 0.0111$). **D–F:** This reduction was rescued by E13.5 in the mutants as assessed by immunohistochemistry and qPCR.

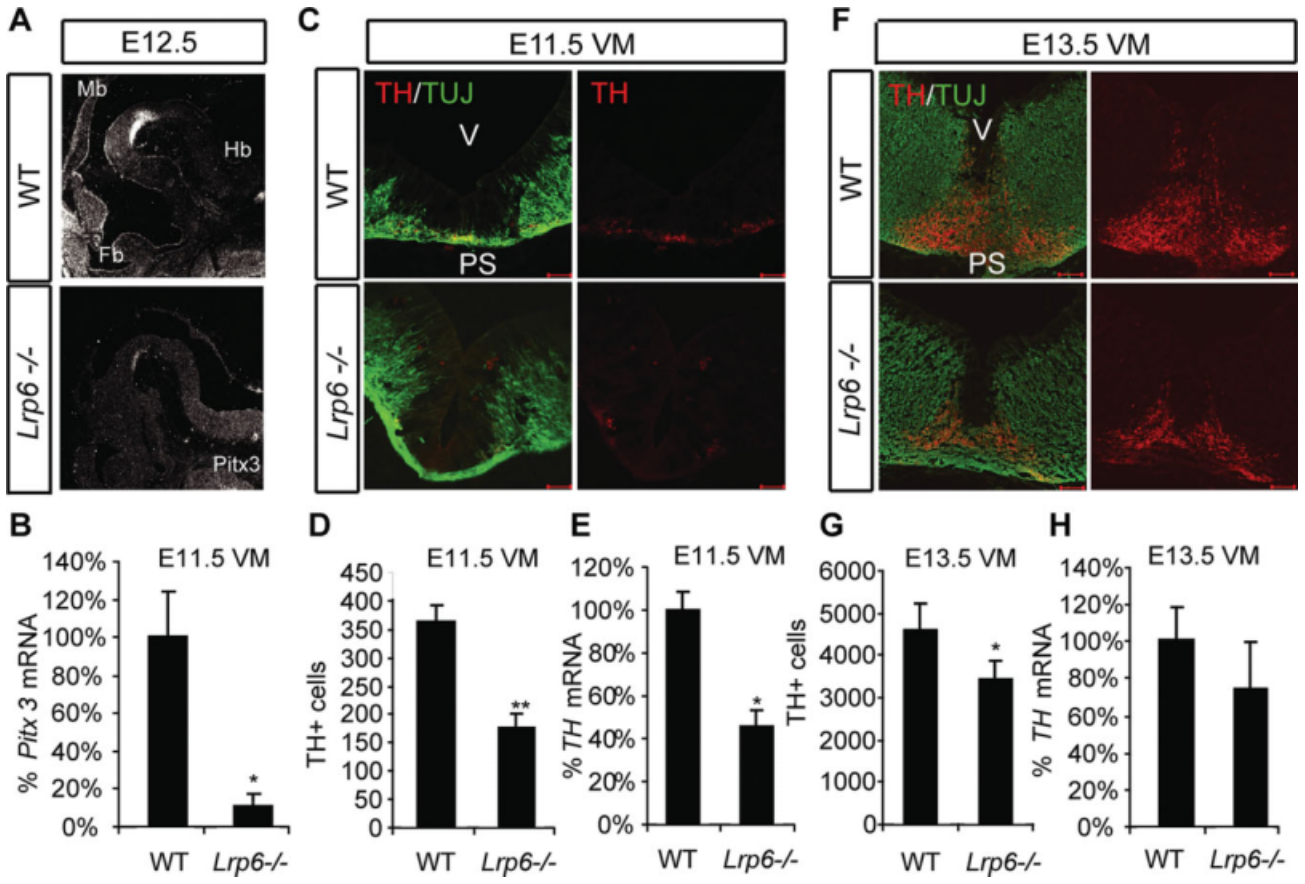

Fig. 6. Delayed onset of dopaminergic (DA) differentiation in *Lrp6*$^{-/-}$ mice. **A,B:** In situ hybridization revealed a drastic reduction of *Pitx3* expression in the *Lrp6*$^{-/-}$ mice at embryonic day (E) 11.5 (A), which was confirmed by qPCR (paired *t*-test; N = 5; *P* = 0.0228) (B). Coronal ventral midbrain (VM) sections of E11.5 wild-type (WT) and *Lrp6*$^{-/-}$ mice revealed a reduced number of tyrosine hydroxylase–positive (TH+) DA neurons in the mutants. **C:** However, overall neuronal differentiation (as assessed by β-tubulin III [TUJ-1]) was not affected. **D:** TH+ cell numbers were reduced from 362.5 ±30.38 in WT to 175.5 ±24.4 in *Lrp6*$^{-/-}$ mice at E11.5 (paired *t*-test; N = 4; *P* = 0.0038). **E:** This reduction was confirmed by qPCR, showing a 50% reduction (paired *t*-test; N = 6; *P* = 0.0120). **F:** A partial recovery in the number of TH+ DA neurons was detected at E13.5 in *Lrp6*$^{-/-}$ mice. **G,H:** TH+ cell numbers were still somewhat reduced in *Lrp6*$^{-/-}$ mice (G), a small difference that could not be detected by qPCR (H).

While the mild similarity of the *Lrp6*$^{-/-}$ mice to the *Wnt1*$^{-/-}$ mice could be expected, based on their similar roles in signaling to β-catenin (Huang and He, 2008), the VM VZ morphogenic phenotype of *Lrp6*$^{-/-}$ mice in relation to *Wnt5a*$^{-/-}$ mice was more surprising. Lrp6 has long been exclusively viewed as a coreceptor for Wnt/β-catenin signaling (Wehrli et al., 2000; He et al., 2004), although recent reports have challenged this view (Tahinci et al., 2007; Bryja et al., 2009). We have previously shown that loss of *Wnt5a* leads to a flattened VM VZ invagination and a rostrocaudally shortened, but laterally expanded DA population (Andersson et al., 2008), morphogenic defects typical of disrupted convergent extension (CE; Ybot-Gonzalez et al., 2007). While the decrease in DA cell numbers in the *Lrp6*$^{-/-}$ mice precluded a detailed analysis of the distribution of DA neurons, analysis of the VM VZ invagination revealed a more narrow, or acute, angle of invagination. It is interesting to note that loss of *Wnt5a* or of *Lrp6* have opposite effects on VM morphology, and that loss of Lrp6 results in neural tube closure defects that are rescued by loss of Wnt5a (Bryja et al., 2009). Overall, this indicates that Wnt5a and Lrp6 functionally oppose each other in VM morphogenesis. Our previous results have shown that Lrp6 physically interacts with Wnt5a and can oppose Wnt5a in regulation of CE (Bryja et al., 2009); however, we have also found that *Wnt5a* and *Lrp6* synergize in some organs or systems (Andersson et al., 2009). Therefore, further studies are warranted to assess whether loss of Lrp6 results in gain-of-function of Wnt5a signaling at the level of DAergic neuron differentiation. At the level of VM progenitor proliferation, loss of *Wnt5a* resulted in an increase in proliferation at E11.5 (Andersson et al., 2008), but we did not detect any difference in proliferation in the *Lrp6*$^{-/-}$ mice.

In summary, our results demonstrate that *Lrp6*$^{-/-}$ mice display a phenotype that is similar to *Wnt1*$^{-/-}$ mice in DA neuron differentiation and opposite to *Wnt5a*$^{-/-}$ mice in midbrain morphogenesis, and that Lrp6 is necessary for the timely onset of DA neuron differentiation in the developing VM. Our results also suggest that other co-receptors may mediate some of the multiple functions regulated by Wnts in the midbrain and specifically in DA neurons.

EXPERIMENTAL PROCEDURES

Lrp6 Mutants and Genotyping

Lrp6$^{+/-}$ mice (Pinson et al., 2000; a kind gift from William Skarnes, The Sanger Institute) were housed, bred, and treated in accordance with the ethical approval for animal experimentation granted by Stockholms Norra Djurförsöks Etiska Nämnd (in Sweden), or by the HMGU Institutional Animal Care and Use Committee (in Germany). WT and heterozygous mice were identified with genotyping PCR reactions with the previously described primers *Lrp6* -U1 and *Lrp6* -D1 (Kelly et al., 2004), and mice with the gene trap insertion were recognized with the following primer set: CD4mix forward: 5′-GCACGGATGTCTCAGAT CAAGAGG-3′ and CD4mix reverse: 5′-CGGGATCATCGCTCCCATATATG-3′, with an annealing temperature of 63°C and an amplicon of 108 bp. For DNA extraction, ear or embryonic tissues were boiled at 95°C for 40 min in 100–200 μl of 25 mM NaOH/0.2 mM ethylenediaminetetraacetic acid (ED TA), after which an equal volume of 40 mM Tris HCl pH 5 was added to neutralize the solution. A total of 3 μl of this solution was used in PCRs, which were performed as described for the qPCR, but without SYBR Green and for 30 cycles.

Noon of the day of plug was taken as E0.5.

Immunohistochemistry and Image Acquisition

E11.5, E13.5, and E17.5 mice were fixed with 4% paraformaldehyde (PFA) overnight and immersed in a 20% sucrose gradient. Samples were then rapidly frozen in Tissue-Tek O.C.T Compound (Labonord, France) on dry ice. Serial sagittal and coronal sections (14 μm thick) were collected on microscope slides (StarFrost, Germany) and stored at −80°C. For immunohistochemistry, slides were thawed and incubated for 10 min with 4% PFA. After three 15 min washes with phosphate-buffered saline (PBS) the slides were blocked with PBTG (PBS with 0.1–0.3% Triton X and 5% goat serum) for 30 min. Primary antibody (rabbit α-TH [1:250-Pelfreeze], rabbit α-Nurr1 [1:1,000-Santa Cruz], rabbit α-active-caspase III [1:100-Cell Signaling] rabbit α-phospho-histone-3 [1:100-Cell Signaling], guinea pig anti-Glast [1:2000, Chemicon], or mouse α-nestin [Rat401, 1:100-Developmental Studies Hybridoma Bank, Iowa]) in PBTG was incubated at 4°C overnight. After three washes with PBS, the sections were again blocked with PBTG for 30 min and incubated for 1–2 hr with secondary antibody (cyanine-2, cyanine-3, or rhodamine-coupled horse-α-mouse IgG 1:200, goat α-rabbit IgG 1:200, or donkey anti-guinea pig 1:500 (Jackson Laboratories)). Slides were then washed three times with PBS for 15 min, counterstained with Hoechst 33258 or DAPI (4′,6-diamidine-2-phenylidole-dihydrochloride; Invitrogen) for 1–20 min, and mounted in PBS/glycerol (1:4). Images were acquired at room temperature with a confocal laser scanning microscope (Zeiss 510, argon (488 nm) and helium-neon (543 and 633 nm) lasers) and Zeiss LSM Viewer software. Images were processed with Adobe Photoshop version 7.0 or CS4. Figure panels were assembled using Adobe Illustrator CS4 or Photoshop CS4.

In Situ Hybridization

WT and *Lrp6*$^{-/-}$ mouse embryos at E11.5, E12.5 and E15.5 were fixed overnight in 4% PFA at 4°C and embedded in paraffin. Serial sections of 8 μm were processed for radioactive in situ hybridization using [S^{35}]-UTP labeled antisense riboprobes. Hybridization was carried out at 56°C in 50% formamide according to a modified protocol of Dagerlind et al. (Dagerlind et al., 1992). Sections were counterstained with Cresyl Violet (Sigma-Aldrich, Sweden). Probes for in situ hybridization were as follows:, *Otx2* (Simeone et al., 1992), *En1* (Davis and Joyner, 1988), *Lmx1b* (Chen et al., 1998), *Shh* (Echelard et al., 1993), *Wnt5a* (Yamaguchi et al., 1999), *Fgf8* (Martinez et al., 1999), *Ngn1*, *Ngn2* (Cau et al., 1997), *TH*, *Pitx3* (kindly given by Jordi Guimera; Brodski et al., 2003), *Lrp5*, *Lrp6* (PCR-products for regions 2884–3444bp for *Lrp5* NM_008513 and 2941–3446bp for *Lrp6* NM_008514 [C. Kokubu]), and *Wnt3a* (Parr et al., 1993).

BrdU and EdU Detection

For proliferation assays, the BrdU Detection kit II and protocol (Roche, Germany) or EdU (Invitrogen) was used with slight modifications. Pregnant mice were injected peritoneally with 5-bromo-2-deoxyuridine (BrdU, 10 μg/g body weight) or 5-ethynyl-2′-deoxyuridine (EdU, Invitrogen, 10 μg/g body weight) 2 hr before sacrificing. For BrdU, embryos/brains were incubated overnight in 4% PFA at 4°C, dehydrated through ethanol and rotihistol and paraffin embedded. Paraffin sections (8 μm) were deparaffinized in rotihistol, rehydrated, cooked in sodium citrate (0.01 M) for 5 min, washed with PBS and incubated 1 hr in blocking solution (PBS with 10% fetal calf serum, 0.05% Triton X-100). Next, slides were incubated overnight at 4°C with anti-BrdU (dilution 1:10 in PBS with 0.05% Triton X-100). After three washes with PBS, sections were incubated 2 hr with the secondary anti-mouse biotinylated antibodies (1:500, Jackson ImmunoResearch). After three washes in PBS, slides were incubated 30 min with ABC solution (ABC-kit, Vectastain, Vector Laboratories) and then diaminobenzidine staining (DAB, Sigma-Aldrich, Sweden) until signal was seen. Slides were washed twice with PBS, dehydrated and mounted with Roti-Histokit (ROTH, Germany).

For EdU staining, embryos/brains were fixed in 4% PFA for 4 hr, washed twice with PBS, and then incubated in 30% sucrose overnight at 4°C. Embryos/brains were then embedded in optimum cutting temperature (O.C.T.) embedding compound on dry ice and 14-μm sections were collected on a cryostat. Slides were rehydrated in PBS before EdU detection, which was performed as described previously (Salic and Mitchison, 2008). In brief, slides were incubated for 30 min with a solution composed of 100 mM Tris (pH 8.5), 1 mM $CuSO_4$, 10 μM Alexa 488 azide (Invitrogen) and 100 mM ascorbic acid. Slides were then washed with PBS and either mounted in glycerol or used for subsequent immunohistochemistry.

TABLE 1. Oligonucleotide Sequences of Primers

mRNA	Annealing temperature (°C)	Sequence (5′-3′)
Lrp5 forward	61	GACATCTACAGCCGGACACTGTTC
Lrp5 reverse		TGGACATTGATAGTGTTGGTGGC
Lrp6 forward	59	GCTACAAATGGCAAAGAGAATGC
Lrp6 reverse		CAGTATACAAGCCATGACCAAACA
TH forward	62	AGTACTTTGTGCGCTTCGAGGTG
TH reverse		CTTGGGAACCAGGGAACCTTG
Nestin forward	59	GTCAGATCGCTCAGATCCTGGA
Nestin reverse		CCAGACTAAGGGACATCTTGAGGT
AHD2 forward	59	GGAAGAAAGAAGGAGCCAAACTG
AHD2 reverse		ACTTCATGATTTGTTGCACTGGTC
Pitx3 forward	65	TTCCCGTTCGCCTTCAACTCG
Pitx3 reverse		GAGCTGGGCGGTGAGAATACAGG

Quantification of Immunohistochemical Data or EdU and Statistical Analyses

Quantitative immunohistochemical data represent means ± standard error of the mean. All the sections where VM was present were counted for each animal and three to four pairs of mice (WT and *Lrp6* mutant) were analyzed. Statistical analysis was performed using Prism 4 software (Graph Pad, San Diego) with paired *t*-test (for littermates) and significance was assumed at the level of $P < 0.05$ ($^*P < 0.05$; ** $0.01 < P < 0.001$; $^{***}P < 0.001$).

For EdU quantification, 3 sections of ventral midbrain were randomly chosen per animal (N = 3 for WT and $Lrp6^{-/-}$ mice) and EdU was quantified within a 2,000μm^2 box within the Glast-expressing floor plate (Fig. 2C). Graphs represent means of three animals per genotype ± standard error of the mean, statistical analyses were performed in Microsoft Excel using a two-tailed unpaired *t*-test and significance was assumed at the level of $P < 0.05$.

Measurement of Ventral Midbrain Ventricular Zone Invagination

WT and $Lrp6^{-/-}$ E11.5 brains were sectioned coronally and stained with DAPI, and images were collected as described above. The angle of VM VZ invagination was measured in ImageJ (Rasband, 1997–2009), as depicted in Figure 3A, in three random sections of ventral midbrain per animal (N = 3 for WT and $Lrp6^{-/-}$ mice). The graph represents means of three animals per genotype ± standard error of the mean, statistical analyses were performed in Microsoft Excel using a two-tailed unpaired *t*-test and significance was assumed at the level of $P < 0.05$ ($^*P < 0.05$).

Reverse Transcription

Total RNA was isolated from pools of VM dissected from E10.5, E11.5, E13.5, E15.5, and postnatal day (P) 1 rats, or from $Lrp6^{-/-}$ or WT E11.5 VMs (n = 6) or E13.5 VMs (n = 3), using RNeasy extraction kit (Qiagen, Hilden, Germany). For RT, 0.25–1 μg of total RNA was initially treated with 1 unit of RQ1 RNAse-free DNAse (Promega, Madison, WI) for 40 min. The DNAse was inactivated by the addition of 1 μl of EDTA 0.02 M and incubated at 65°C for 10 min. A total of 1.5 μg random primers (Invitrogen) were then added, and the mixture was incubated at 65°C for 5 min. Each sample was then divided equally into two tubes, a cDNA reaction tube and a negative control tube (RT−). A master mix containing 1× First-Strand Buffer (Invitrogen), 0.01 M dithiothreitol (DTT; Invitrogen), and 0.5 mM dNTPS (Promega) was then added to both cDNA and RT− tubes and incubated at 25°C for 10 min, followed by a 2-min incubation at 42°C. Supercript II reverse transcriptase (200 units, Invitrogen) was then added only to the cDNA tubes and all samples were incubated at 42°C for 50 min. Superscript II was inactivated by incubation for 10 min at 70°C. Both cDNA and RT- were then diluted 10 times, for further analysis.

Primer Design and Quantitative PCR

Genbank cDNA sequences were used to design gene specific primers in Primer Express 2.0 (PE Applied Biosystems, CA). The specificity of PCR primers was determined by BLAST run of the primer sequences. The oligonucleotide sequences for the primers are displayed in Table 1 and their annealing temperature is 59/60°C, unless otherwise indicated. Apart from Quantum RNA classic 18S internal standard (Ambion, Austin, TX), all primers were purchased from DNA Technologies, Denmark.

qPCR reactions were performed twice for a particular gene, in triplicate (or duplicate) for each sample. Each PCR reaction had a final volume of 25 μl and was derived from 75-μl (50-μl) master mixes containing 3 μl (2 μl) of 10×-diluted cDNA or RT−. Each PCR reaction consisted of 1× PCR buffer (Invitrogen), 3 mM $MgCl_2$ (Invitrogen), 0.2 mM dNTPs (Promega, Madison), 0.3 μM of each of the forward and reverse primers, 0.5 unit Platinum *Taq* DNA polymerase (Invitrogen) and 1× SYBR Green (Molecular Probes, Leiden, The Netherlands). The following thermo cycling program was used: 94°C for 2 min and then for 35–40 cycles 94° C for 30 sec, 60°C for 30 sec, 72° C for 15 sec, and at 80°C for 5 sec (for SYBR Green detection), on the ABI PRISM 5700 Detection System (PE Applied Biosystems, Foster City, CA). Alternatively, the Platinum Quantitative PCR SuperMix-UDG (Invitrogen) was used, according to the manufacture's instructions (but with a 4× dilution from the original mastermix, instead of 2×). Random PCR products were also run in a 2% agarose gel to verify the size of the amplicon.

Standard curves were generated for every real-time PCR run and were obtained by using serial three-fold dilutions of a sample containing the sequence of interest (reverse transcribed RNA, plasmid containing sequence or genomic DNA). Their plots were used to convert Cts (number of PCR cycles needed for a given template to be amplified to an

established fluorescence threshold) into arbitrary quantities of initial template for a given sample. The expression levels were then obtained by subtracting the RT− value for each sample from the corresponding cDNA value (when appropriate), and subsequently normalized by the value of the housekeeping gene, 18S, obtained for every sample in parallel assays. The 18S assays were run at the beginning and in the middle of assays, to verify the integrity of the samples.

Statistical analysis of the qPCR results was performed by paired *t*-test. Significance for all tests was assumed at the level of $P < 0.05$ ($^{*}P < 0.05$; $^{**}P < 0.001$; $^{***}P < 0.0001$).

ACKNOWLEDGMENTS

We thank Drs. Anita Hall, Ola Hermanson, Kenji Imai, and Ulrich Heinzmann for critical reading and advice and Lottie Jansson-Sjostrand, Lenka Bryjova, Lena Amaloo, Johnny Söderlund, Claudia Tello, and Susanne Laass for additional assistance. We thank Drs. Kathy Pinson (Berkeley) and William Skarnes (The Sanger Institute), for the *Lrp6*$^{-/-}$ mice. E.A. was funded by grants from the Swedish Foundation for Strategic Research (INGVAR and CEDB), Swedish Research Council (DBRM), Norwegian Research Council, Karolinska Institutet, Michael J. Fox Foundation, and European Commission (Eurostemcell). G.C.B. is supported by the Portuguese Fundação para a Ciência e Tecnologia, Karolinska Institute and Calouste Gulbenkian Foundation. The Work of W.W. and N.P. is supported by BMBF National Genome Research Network (NGFN+ Functional Genomics of Parkinson Disease), Virtual Institute on Neurodegeneration and Ageing, the Initiative and Networking Fund in the framework of the Helmholtz Alliance of Systems Biology and of Mental Health in an Ageing Society, Bayerischer Forschungsverbund 'ForNeuroCell', European Union, and Deutsche Forschungsgemeinschaft.

REFERENCES

Andersson ER, Prakash N, Cajanek L, Minina E, Bryja V, Bryjova L, Yamaguchi TP, Hall AC, Wurst W, Arenas E. 2008. Wnt5a Regulates Ventral Midbrain Morphogenesis and the Development of A9-A10 Dopaminergic Cells In Vivo. PLoS ONE 3:e3517.

Andersson E, Bryjova L, Biris K, Yamaguchi TP, Arenas E, Bryja V. 2009. Genetic interaction between Lrp6 and Wnt5a during mouse development. Dev Dyn 239:237–245.

Brodski C, Weisenhorn DM, Signore M, Sillaber I, Oesterheld M, Broccoli V, Acampora D, Simeone A, Wurst W. 2003. Location and size of dopaminergic and serotonergic cell populations are controlled by the position of the midbrain-hindbrain organizer. J Neurosci 23:4199–4207.

Bryja V, Andersson ER, Schambony A, Esner M, Bryjova L, Biris KK, Hall AC, Kraft B, Cajanek L, Yamaguchi TP, Buckingham M, Arenas E. 2009. The extracellular domain of Lrp5/6 inhibits noncanonical Wnt signaling in vivo. Mol Biol Cell 20:924–936.

Castelo-Branco G, Wagner J, Rodriguez FJ, Kele J, Sousa K, Rawal N, Pasolli HA, Fuchs E, Kitajewski J, Arenas E. 2003. Differential regulation of midbrain dopaminergic neuron development by Wnt-1, Wnt-3a, and Wnt-5a. Proc Natl Acad Sci U S A 100: 12747–12752.

Castelo-Branco G, Rawal N, Arenas E. 2004. GSK3 beta inhibition/beta-catenin stabilization in ventral midbrain precursors increases differentiation of dopamine neurons. J Cell Sci 117: 5731–5737.

Castillo SO, Baffi JS, Palkovits M, Goldstein DS, Kopin IJ, Witta J, Magnuson MA, Nikodem VM. 1998. Dopamine biosynthesis is selectively abolished in substantia nigra/ventral tegmental area but not in hypothalamic neurons in mice with targeted disruption of the Nurr1 gene. Mol Cell Neurosci 11: 36–46.

Cau E, Gradwohl G, Fode C, Guillemot F. 1997. Mash1 activates a cascade of bHLH regulators in olfactory neuron progenitors. Development 124:1611– 1621.

Chen H, Lun Y, Ovchinnikov D, Kokubo H, Oberg KC, Pepicelli CV, Gan L, Lee B, Johnson RL. 1998. Limb and kidney defects in Lmx1b mutant mice suggest an involvement of LMX1B in human nail patella syndrome. Nat Genet 19:51–55.

Ciani L, Salinas PC. 2005. WNTS in the vertebrate nervous system: from patterning to neuronal connectivity. Nat Rev Neurosci 6:351–362.

Cong F, Schweizer L, Varmus H. 2004. Wnt signals across the plasma membrane to activate the β-catenin pathway by forming oligomers containing its receptors, Frizzled and LRP. Development 131:5103–5115.

Dagerlind A, Friberg K, Bean AJ, Hokfelt T. 1992. Sensitive mRNA detection using unfixed tissue: combined radioactive and non-radioactive in situ hybridization histochemistry. Histochemistry 98:39–49.

Danielian PS, McMahon AP. 1996. Engrailed-1 as a target of the Wnt-1 signalling pathway in vertebrate midbrain development. Nature 383:332–334.

Davis CA, Joyner AL. 1988. Expression patterns of the homeo box-containing genes En-1 and En-2 and the proto-oncogene int-1 diverge during mouse development. Genes Dev 2:1736–1744.

Echelard Y, Epstein DJ, St-Jacques B, Shen L, Mohler J, McMahon JA, McMahon AP. 1993. Sonic Hedgehog, a member of a family of putative signaling molecules, is implicated in the regulation of CNS polarity. Cell 75:1417–1430.

Fischer T, Guimera J, Wurst W, Prakash N. 2007. Distinct but redundant expression of the Frizzled Wnt receptor genes at signaling centers of the developing mouse brain. Neuroscience 147:693–711.

He X, Semenov M, Tamai K, Zeng X. 2004. LDL receptor-related proteins 5 and 6 in Wnt/beta-catenin signaling: arrows point the way. Development 131:1663–1677.

Houston DW, Wylie C. 2002. Cloning and expression of Xenopus Lrp5 and Lrp6 genes. Mech Dev 117:337–342.

Huang H, He X. 2008. Wnt/beta-catenin signaling: new (and old) players and new insights. Curr Opin Cell Biol 20: 119–125.

Hwang DY, Ardayfio P, Kang UJ, Semina EV, Kim KS. 2003. Selective loss of dopaminergic neurons in the substantia nigra of Pitx3-deficient aphakia mice. Brain Res Mol Brain Res 114:123–131.

Kele J, Simplicio N, Ferri AL, Mira H, Guillemot F, Arenas E, Ang SL. 2006. Neurogenin 2 is required for the development of ventral midbrain dopaminergic neurons. Development 133:495–505.

Kelly OG, Pinson KI, Skarnes WC. 2004. The Wnt co-receptors Lrp5 and Lrp6 are essential for gastrulation in mice. Development 131:2803–2815.

Le W, Conneely OM, Zou L, He Y, Saucedo-Cardenas O, Jankovic J, Mosier DR, Appel SH. 1999. Selective agenesis of mesencephalic dopaminergic neurons in Nurr1-deficient mice. Exp Neurol 159:451–458.

Logan CY, Nusse R. 2004. The Wnt signaling pathway in development and disease. Annu Rev Cell Dev Biol 20:781–810.

Mao J, Wang J, Liu B, Pan W, Farr GH, 3rd, Flynn C, Yuan H, Takada S, Kimelman D, Li L, Wu D. 2001. Low-density lipoprotein receptor-related protein-5 binds to Axin and regulates the canonical Wnt signaling pathway. Mol Cell 7:801–809.

Martinez S, Crossley PH, Cobos I, Rubenstein JL, Martin GR. 1999. FGF8 induces formation of an ectopic isthmic organizer and isthmocerebellar development via a repressive effect on Otx2 expression. Development 126:1189–1200.

Maxwell SL, Ho HY, Kuehner E, Zhao S, Li M. 2005. Pitx3 regulates tyrosine hydroxylase expression in the substantia nigra and identifies a subgroup of mesencephalic dopaminergic progenitor neurons during mouse development. Dev Biol 282:467–479.

McMahon AP, Bradley A. 1990. The Wnt-1 (int-1) proto-oncogene is required for development of a large region of the mouse brain. Cell 62:1073–1085.

Nunes I, Tovmasian LT, Silva RM, Burke RE, Goff SP. 2003. Pitx3 is required for development of substantia nigra dopaminergic neurons. Proc Natl Acad Sci U S A 100:4245–4250.

Panhuysen M, Vogt Weisenhorn DM, Blanquet V, Brodski C, Heinzmann U, Beisker W, Wurst W. 2004. Effects of Wnt1 signaling on proliferation in the developing mid-/hindbrain region. Mol Cell Neurosci 26:101–111.

Parr BA, Shea MJ, Vassileva G, McMahon AP. 1993. Mouse Wnt genes exhibit discrete domains of expression in the early embryonic CNS and limb buds. Development 119:247–261.

Pinson KI, Brennan J, Monkley S, Avery BJ, Skarnes WC. 2000. An LDL-receptor-related protein mediates Wnt signalling in mice. Nature 407:535–538.

Prakash N, Brodski C, Naserke T, Puelles E, Gogoi R, Hall A, Panhuysen M, Echevarria D, Sussel L, Weisenhorn DM, Martinez S, Arenas E, Simeone A, Wurst W. 2006. A Wnt1-regulated genetic network controls the identity and fate of midbrain-dopaminergic progenitors in vivo. Development 133:89–98.

Qian D, Jones C, Rzadzinska A, Mark S, Zhang X, Steel KP, Dai X, Chen P. 2007. Wnt5a functions in planar cell polarity regulation in mice. Dev Biol 306: 121–133.

Rasband WS. 1997–2005. ImageJ. Bethesda, MD: US National Institutes of Health.

Rawal N, Castelo-Branco G, Sousa K, Kele J, Kobayashi K, Okano H, Arenas E. 2006. Spatial and temporal expression dynamics of Wnt signaling components in the developing midbrain. Exp Cell Res 312:1626–1636.

Salic A, Mitchison TJ. 2008. A chemical method for fast and sensitive detection of DNA synthesis in vivo. Proc Natl Acad Sci U S A 105:2415–2420.

Simeone A, Acampora D, Gulisano M, Stornaiuolo A, Boncinelli E. 1992. Nested expression domains of four homeobox genes in developing rostral brain. Nature 358:687–690.

Smidt MP, van Schaick HS, Lanctot C, Tremblay JJ, Cox JJ, van der Kleij AA, Wolterink G, Drouin J, Burbach JP. 1997. A homeodomain gene Ptx3 has highly restricted brain expression in mesencephalic dopaminergic neurons. Proc Natl Acad Sci U S A 94: 13305–13310.

Smidt MP, Smits SM, Bouwmeester H, Hamers FP, van der Linden AJ, Hellemons AJ, Graw J, Burbach JP. 2004. Early developmental failure of substantia nigra dopamine neurons in mice lacking the homeodomain gene Pitx3. Development 131:1145–1155.

Tahinci E, Thorne CA, Franklin JL, Salic A, Christian KM, Lee LA, Coffey RJ, Lee E. 2007. Lrp6 is required for convergent extension during Xenopus gastrulation. Development 134:4095–4106.

Tamai K, Semenov M, Kato Y, Spokony R, Liu C, Katsuyama Y, Hess F, Saint-Jeannet JP, He X. 2000. LDL-receptor-related proteins in Wnt signal transduction. Nature 407:530–535.

Thomas KR, Capecchi MR. 1990. Targeted disruption of the murine int-1 proto-oncogene resulting in severe abnormalities in midbrain and cerebellar development. Nature 346:847–850.

van den Munckhof P, Luk KC, Ste-Marie L, Montgomery J, Blanchet PJ, Sadikot AF, Drouin J. 2003. Pitx3 is required for motor activity and for survival of a subset of midbrain dopaminergic neurons. Development 130:2535–2542.

Viti J, Gulacsi A, Lillien L. 2003. Wnt regulation of progenitor maturation in the cortex depends on Shh or fibroblast growth factor 2. J Neurosci 23:5919–5927.

Wallen A, Zetterstrom RH, Solomin L, Arvidsson M, Olson L, Perlmann T. 1999. Fate of mesencephalic AHD2-expressing dopamine progenitor cells in NURR1 mutant mice. Exp Cell Res 253: 737–746.

Wehrli M, Dougan ST, Caldwell K, O'Keefe L, Schwartz S, Vaizel-Ohayon D, Schejter E, Tomlinson A, DiNardo S. 2000. arrow encodes an LDL-receptor-related protein essential for Wingless signalling. Nature 407:527–530.

Yamaguchi TP, Bradley A, McMahon AP, Jones S. 1999. A Wnt5a pathway underlies outgrowth of multiple structures in the vertebrate embryo. Development 126:1211–1223.

Ybot-Gonzalez P, Savery D, Gerrelli D, Signore M, Mitchell CE, Faux CH, Greene ND, Copp AJ. 2007. Convergent extension, planar-cell-polarity signalling and initiation of mouse neural tube closure. Development 134:789–799.

Zetterstrom RH, Solomin L, Jansson L, Hoffer BJ, Olson L, Perlmann T. 1997. Dopamine neuron agenesis in Nurr1-deficient mice. Science 276:248–250.

Zhou CJ, Pinson KI, Pleasure SJ. 2004a. Severe defects in dorsal thalamic development in low-density lipoprotein receptor-related protein-6 mutants. J Neurosci 24:7632–7639.

Zhou CJ, Zhao C, Pleasure SJ. 2004b. Wnt signaling mutants have decreased dentate granule cell production and radial glial scaffolding abnormalities. J Neurosci 24:121–126.